Khadem-Reza and Zare
Middle East Current Psychiatry (2022) 29:54
https://doi.org/10.1186/s43045-022-00220-1

Middle East Current Psychiatry

RESEARCH

Open Access

Automatic detection of autism spectrum disorder (ASD) in children using structural magnetic resonance imaging with machine vision system

Zahra Khandan Khadem-Reza and Hoda Zare*

Abstract

Background: Autism spectrum disorder (ASD) is a group of developmental disorders of the nervous system whose main manifestations are defects in social interactions, communication, repetitive behaviors, and limited interests. Over the years, the use of magnetic resonance imaging (MRI) to help identify patterns that are common in people with autism has increased for classification purposes. This study propose a method for classifying ASD patients versus controls using structural MRI information. In order to increase the accuracy of this method, the volume and surface features of the structural images are used simultaneously.

Results: The accuracy of diagnosis respectively was 86.29%, 71.15%, 86.53%, and 88.46% with SVM, RF, KNN, and ANN classifiers. The highest accuracy of diagnosis was obtained using ANN.

Conclusions: Since clinical evaluations for the diagnosis of autism are extremely time-consuming and depend on the expertise of a specialist, the importance of intelligent diagnosis of this disorder becomes clear. The aim of this study was to design an intelligent system to diagnose autism spectrum disorder.

Keywords: ASD, Children, sMRI, Machine vision

Background

Autism spectrum disorder (ASD) represents a cluster of relatively common developing disorders that faces social communication difficulties, social determination, and limited repetitive-behavioral patterns. Autism is one of the major problems in children, and it has recently been shown that approximately 1 out of 68 children deals with it [1]. Traditionally, these disorders have been diagnosed using interview-based methods, such as the Autism Diagnostic Survey [2] and the revised Autism Diagnostic Interview [3]. Although these methods are flawed and also unable to assess any biological cause behind the observed behavioral symptoms, they can be useful for treatment and even for prevention. To overcome these problems, brain-based imaging techniques are being considered as an alternative diagnostic tool. Magnetic resonance imaging (MRI) is an important brain imaging technique that provides high-resolution information about the structure, composition, and function of the brain. Some studies have attempted to extract features that show differences in brain structures and use machine learning techniques to classify autistic people from control people.

Singh et al. separated an autistic group from controls using structural magnetic resonance imaging. This was done using a new algorithm and only by examining the cerebral cortex and achieved a high classification accuracy of 90% using the LPboost algorithm [4]. Ecker et al.

*Correspondence: ZareH@mums.ac.ir

Department of Medical Physics, Faculty of Medicine, Mashhad University of Medical Sciences, Mashhad 9137913316, Iran

used whole-brain structural magnetic resonance imaging to classify autistic children from the control group. SVM was used for classification and achieved the highest sensitivity and specificity of 90% and 80% [5]. Jiao et al. developed a model for predicting ASD based on cortical thickness in different areas of the brain. The study achieved a log accuracy of 87% using the Logistic Model Tree Classifier (LMT) [6]. Katuwal et al. predicted the ability of structural MRI to diagnose ASD. Finally, this study achieved the highest accuracy of 67% in ASD detection [7]. Ismail et al. introduced a new computer-aided diagnosis system based on shape using structural MRI to identify autism at various stages of life. The system is designed using the ABIDE database and showed 93% accuracy [8]. Xiao et al. developed a model for diagnosing ASD using features extracted from structural MRI using machine learning. The model was designed using the RF classification and with the help of the cortical thickness feature of the average area of the brain, and it achieved 88% accuracy [9]. Khalil et al. designed a computer system to diagnose ASD using shape features extracted from structural MRI and using ABIDE database images and a multilevel deep network. They achieved an accuracy of 93% [10].

The purpose of this study is automatic detection of autism spectrum disorder (ASD) in children using features extracted from structural images. In order to achieve higher accuracy in diagnosing autism, surface and volume features are used simultaneously for classification.

Method

The steps of the proposed method are shown in Fig. 1.

Subjects

In this study, structural data from magnetic resonance images from the Autism Brain Imaging Data Exchange (ABIDII) were used. We used structural magnetic resonance imaging from the Langone Medical Center, NYU: site 1 model (NYU). Image data in this study is achieved from 26 autistic subject and 26 healthy control aged 5 to 10 years. The demographic for the participants is proven in Table 1.

MRI acquisition

Magnetic resonance images were acquired using a Siemens 3T scanner in the Neuroimaging Information Technology Initiative (NIFTI) format with the following protocol: repetition time and echo time = 3.25 ms, rotation angle = 7°, plane resolution = 1.3 mm × 1 mm, 1.3 mm slice thickness in 0.665 mm gap, 128 slices, 256 mm × 256 mm field of view, and acquisition time = 8:07 min.

Preprocessing and segmentation

The CAT12 and SPM12 toolkits in MATLAB R2019a software version are used for structural brain imaging. We performed preprocessing and segmentation steps using the CAT12 toolbox with appropriate default settings. Nonlinear record is corrected for displacement field uniformity and then images segmented into GM, WM, and CSF components [11]. We used the Diffeomorphic Anatomical Registration Algorithm via Exponential Lie Algebra (DARTEL) to normalize the segmented scans to the standard MNI space [12]. The image of the main stages of preprocessing is shown in Fig. 2, and the segmented image into white matter, gray matter, and cerebrospinal fluid is also shown in Fig. 3.

Brain reconstruction

Surface reconstruction steps are performed using CAT12 toolbox in MATLAB R2019a software. We use

Table 1 Demographics for the participants

	ASD ($n = 26$) Mean (SD)	**HC ($n = 26$) Mean (SD)**	***p*-value (*)**
Age	7.12 (0.98)	7.48 (1.39)	0.320
Sex	24 M/2 F	25 M/1 F	0.584

ASD autism spectrum disorder, *HC* healthy controls, *M* male, *F* female. $p < 0.05$ was considered statistically significant

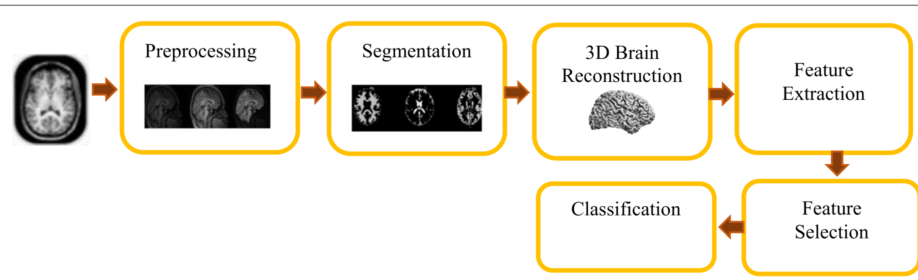

Fig. 1 Steps performed in the study. (The proposed method)

a fully automated method that allows for the measurement of cortical thickness and reconstructions of the central surface in one step. It uses a tissue segmentation to estimate the white matter (WM) distance and then projects the local maxima (which is equal to the cortical thickness) to other gray matter voxels by using a neighbor relationship described by the WM distance [13]. Then topological correction is performed with the aim of repairing topological defects using a method containing spherical harmonics that allows direct correction of defects on the brain surface mesh [14]. The spherical map is used to create a common coordinate system. The reconstructed surface in the CAT12 toolbox is shown in Fig. 4.

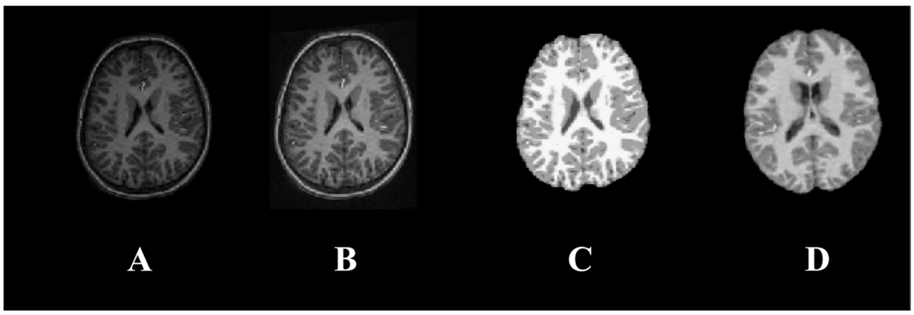

Fig. 2 Stages of preprocessing of structural images of the brain. **A** Initial image. **B** Image after intensity normalization. **C** Segmented image with skull removal. **D** Image after spatial normalization in DARTEL-modified space based on MNI. (The image of the main stages of preprocessing)

Fig. 3 Segmented images. **A** Original image. **B** White matter of the brain. **C** Gray matter of the brain. (The segmented image into white matter, gray matter, and cerebrospinal fluid)

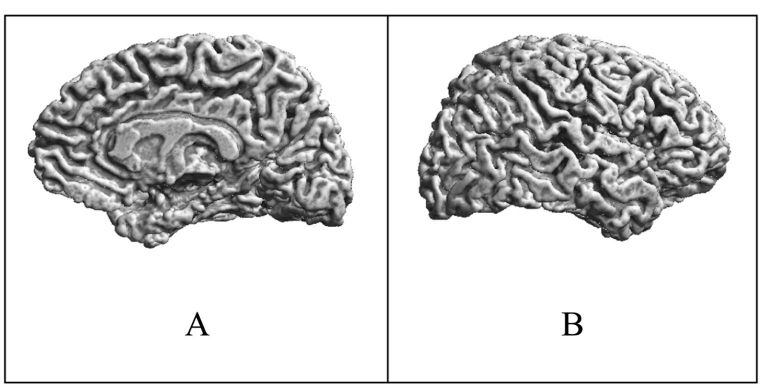

Fig. 4 Reconstructed surface by CAT12 toolbox. **A** Reconstruction of internal surface of right hemisphere surface of the brain. **B** Reconstruction of external surface of left hemisphere surface of the brain. (The reconstructed surface in the CAT12 toolbox)

Feature extraction

Extraction of structural magnetic resonance image features using CAT12 toolbox is done in two steps:

1) Extraction of volume-related features: Volume-related features include volumetric measurement of brain tissue (white matter, gray matter, and cerebrospinal fluid), absolute intracranial volume, and volumetric measurement of white matter and gray matter of the brain in 68 Hammers atlas regions.
2) Extraction of surface-related features: Surface-related features include average and standard deviation of cerebral cortex thickness and calculation of cerebral cortex thickness parameters, surface complexity (fractal dimension), sulcus depth, and gyrification index in 68 Desikan-Killiany (DK) atlas regions.

The volume and surface features extracted from the structural magnetic resonance images are given separately in Table 2.

A feature matrix is then constructed for the extracted features for each autism and control group. The dimensions of the feature matrices related to the structural magnetic resonance images for each group are given in Table 3. The dimensions of the final feature matrix for each group are estimated to be 26 × 414, and the feature matrix for intergroup classification is constructed with dimensions of 52 × 414. Dimensions of feature matrices related to structural magnetic resonance imaging are given in Table 3.

Table 3 Dimensions of feature matrices related to structural magnetic resonance imaging

Features in each group	Matrix size
Volumetric measurement of brain tissues	4 × 26
Volumetric measurements of white and gray matter in the Hammers atlas regions	2 × 68 × 26
Mean and standard deviation of cerebral cortex thickness	2 × 26
Surface and brain shape parameters in the DK atlas regions	4 × 68 × 26
Total	414 × 26

Feature selection

The FCBF method (fast correlation-based feature selection) in Python software was used to select the basic features of group segregation before classification to eliminate inappropriate features and increase the accuracy of machine vision.

Classification

Automated classification using structural magnetic resonance imaging is performed using four machine vision algorithms including support vector machine algorithms, random forest, nearest neighbor, and artificial neural network with tenfold cross-validation (K fold = 10) in Python 3.8.3 software. The value of K in KNN algorithm is equal to 3, and the number of hidden layers of ANN algorithm is considered 3. The output of classification algorithms is a confusion matrix that can be used to evaluate the algorithm. Finally, the performance of all four classifications is evaluated, and the best performance of this system in intergroup classification is calculated.

Results

Feature selection results

The selected features by the FCBF algorithm are listed in Table 4.

Table 2 Volume and surface features extracted from the structural magnetic resonance images

Features	Description	
Volume	WMV T	White matter volume total
	GMV T	Gray matter volume total
	CSFV T	Cerebrospinal fluid volume total
	TIV	Total intracranial volume
	WMVH n ($n = 1{:}68$)	White matter volume per Hammers atlas
	GMVH n ($n = 1{:}68$)	Gray matter volume per Hammers atlas
Surface	Mean CT	Mean cortical thickness per DK atlas
	SD CT	Standard deviation cortical thickness per DK atlas
	CTDK n ($n = 1{:}68$)	Cortical thickness per DK atlas
	CCDK n ($n = 1{:}68$)	Cortical complexity per DK atlas
	SDDK n ($n = 1{:}68$)	Sulcus depth per DK atlas
	GIDK n ($n = 1{:}68$)	Gyrification index per DK atlas

Table 4 Selected features by the FCBF algorithm

Feature	Description
WMVH 3	White matter volume of L amygdala
WMVH 4	White matter volume of R amygdala
WMVH 5	White matter volume of L anterior medial temporal lobe
WMVH 39	White matter volume of L putamen
WMVH 42	Gray matter volume of R thalamus
GMVH 16	Gray matter volume of R fusiform gyrus
GMVH 45	Corpus callosum gray matter volume of L
SD CT	Standard deviation cortical thickness
CTDK 7	Cortical thickness of L cuneus
CTDK 58	Cortical thickness of R superior temporal
CCDK 40	Cortical complexity of R pericalcarine
SDDK 50	Sulcus depth of R rostral anterior cingulate

Table 5 Confusion matrix components obtained from each of the classification algorithms based on the properties selected from the structural magnetic resonance images

	TP	TN	FP	FN
SVM	22	21	5	4
RF	17	20	6	9
KNN	22	23	3	4
ANN	25	21	5	1

TP true positive, *TN* true negative, *FP* false positive, *FN* false negative

Table 6 Evaluation parameters of classification systems based on selected features from structural magnetic resonance images

	Specificity (%)	Sensitivity (%)	Precision (%)	Accuracy (%)
SVM	80.76	84.61	81.48	82.69
RF	76.92	65.38	73.91	71.15
KNN	88.46	84.61	88.00	86.53
ANN	80.76	96.15	83.33	88.46

Classification results

The components of the confusion matrix resulting from each of the classification algorithms are given in Table 5. Evaluation parameters for each classification system are also calculated in Table 6.

According to the results, the automated classification of the artificial neural network has the best performance compared to other algorithms for categorizing the autism group and the control one and with 88.46% accuracy, which is able to distinguish between these two groups.

Discussion

Nearly two-hundred studies over the past 20 years have planned general anatomy changes of ASD, and several other ones among them have more explored the chance to utilize these markers to get prognosticative models. To this point, completely different sorts of neuroimaging feature are applied as diagnostic predictor. Structural features enclosed brain volume (white matter, gray matter, and total brain) [15] and morphological features (average convexity or concavity, mean curvature, metric distortion, cortical thickness, metric distortion, cortical surface, and cortical volume) [4–6].

We compared the four popular machine-learning classifiers, including support vector machine (SVM), random forest (RF), nearest neighbor (KNN) algorithm, and artificial neural network (ANN) to evaluate the performance shown in generating the diagnostic models of ASD. We found ANN superior to the other three classifiers. According to Table 6 in the present study, SVM, RF, KNN, and ANN achieved 82.69%, 71.15%, 86.53%, and 88.46% accuracy respectively in the classification and diagnosis of ASD using structural magnetic resonance imaging. We arrived at a conclusion that ANN was the optimal approach for neuroimaging data mining in a small sample size. Table 7 shows the performance of the machine vision system using structural magnetic resonance imaging in past and present studies. According to this table, although the accuracy of the present study is

Table 7 Performance of the machine vision system using structural magnetic resonance imaging in past studies and present study

Performance	Classification algorithm	Study
90% accuracy	LPboost algorithm	Singh et al. [4]
90% highest sensitivity	SVM	Ecker et al. [5]
87% accuracy	LMT	Jiao et al. [6]
67% highest accuracy	SVM, RF, GBM	Katuwal et al. [7]
93% accuracy	Multilevel deep network	Ismail et al. [8]
88% accuracy	RF	Xiao et al. [9]
93% accuracy	Multilevel deep network	Khalil et al. [10]
88/46% highest accuracy with ANN	SV, RF, KNN ,ANN	Present study

lower than several studies, with considering the number of people studied and their age range, it has acceptable accuracy.

Although the accuracy of the present study is lower than several studies, with considering the number of people studied and their age range, it has acceptable accuracy.

Autism spectrum disorder (ASD) and attention-deficit hyperactivity disorder (ADHD) frequently co-occur. Exact comorbidity rates are not well known due to the DSM-IV restriction of diagnosing ASD and ADHD in the same individual [16]. There are articles for application of structural magnetic resonance in the diagnosis of ADHD or intellectual disability [17–24]. According to these studies, features such as the thickness of the cerebral cortex and the volume of different areas of the brain along with the volume of white and gray matter are biomarkers of diagnosis ADHD, and that these features are also known as biomarkers in ASD patients in this study. But the Sulcus depth feature, which is one of the biomarkers of autism diagnosis in this study, has not been used as a biomarker in any of the diagnostic studies of ADHD. The sulcus depth in different areas of the brain seems to be one of the features that changes in ASD patients compared to healthy subjects, but in ADHD patients, this change is not observed. Finally, the designed algorithm in this study can be used to diagnose ADHD using structural images, and its results can be compared with the present study in terms of the type of extraction features. This comparison can help differentiate these two disorders.

It is prompt that the study be performed for higher accuracy with the higher quantity of data. Also, it may be organized by data from ASD and HC groups with younger age. Different ways of analyzing structural resonance imaging ought to even be ascertained. This analysis has targeted on the structure of the brain. In future researches, additionally to structural images of the brain, different brain imaging modalities like functional magnetic resonance imaging and DTI may be used for automatic detection. Other intelligent detection algorithms can even be used.

Limitation

Autism spectrum disorder is an extremely heterogenous disorder, where any of the selected patients suffered from associated low IQ, delayed speech, epilepsy, or any other forms of comorbidities. These comorbidities can affect the volume and surface of the brain, which can affect the specificity of the diagnosis. Since there is no information about diseases associated with autism in selected patients, this problem is one of the limitations of the present study.

Conclusions

The proposed framework was tested on 52 subjects of ABIDE data set consisting of 26 patients with ASD and 26 controls. Since clinical evaluations for the diagnosis of autism are extremely time-consuming and depend on the expertise of a specialist, the importance of intelligent diagnosis of this disorder becomes clear. The aim of this study was to design an intelligent system to diagnose this disorder. This study reached the highest diagnostic accuracy of 88.46% using the ANN classification, which is a significant result. To conclude, this paper proposed an autism diagnosis approach that analyzes the brain's local areas, which could help understand the autism spectrum disorder.

Abbreviations

ASD: Autism spectrum disorder; MRI: Magnetic resonance imaging; SVM: Support vector machine; RF: Random forest; KNN: Nearest neighbor; ANN: Artificial neural network; ABIDE: Autism Brain Imaging Data Exchange; HC: Healthy controls; NIFTI: Neuroimaging Information Technology Initiative; CAT: Computational anatomy toolbox; SPM: Statistical parametric mapping; DARTEL: Diffeomorphic Anatomic Registration Through Exponentiated Lie algebra algorithm; MNI: Montreal Neurological Institute; GM: Gray matter; WM: White matter; CSF: Cerebrospinal fluid; LMT: Logistic model tree; GBM: Gradient boosting machine; DK: Desikan-Killiany; ADHD: Attention-deficit hyperactivity disorder; DTI: Diffusion tensor imaging.

Acknowledgements

This paper was extracted from a M.S.c thesis of Medical Physics. The authors would like to thank the Research Deputy of MUMS for financial support of this project, numbered (980858). Ethics code: IR.MUMS.MEDICAL.REC.1398.717).

Authors' contributions

HZ contributed as a research assistant as well as a technical advisor. ZK was a major contributor to image analyzing and writing the manuscript. The authors read and approved the final manuscript.

Funding

The Research Deputy of Mashhad University of Medical Sciences financially supported this research in terms of M.Sc. dissertation.

Availability of data and materials

The datasets used and/or analyzed during the current study are available from the corresponding author on reasonable request.

Declarations

Ethics approval and consent to participate

Not applicable

Consent for publication

Not applicable

Competing interests

The authors declare that they have no competing interests.

Received: 14 April 2022 Accepted: 4 June 2022
Published online: 19 July 2022

References

1. Idring S et al (2015) Changes in prevalence of autism spectrum disorders in 2001–2011: findings from the Stockholm youth cohort. J Autism Dev Disord 45(6):1766–1773
2. Lord C et al (1989) Austism diagnostic observation schedule: a standardized observation of communicative and social behavior. J Autism Dev Disord 19(2):185–212

3. Lord C, Rutter M, Le Couteur A (1994) Autism diagnostic interview-revised: a revised version of a diagnostic interview for caregivers of individuals with possible pervasive developmental disorders. J Autism Dev Disord 24(5):659–685
4. Singh V, Mukherjee L, Chung MK (2008) Cortical surface thickness as a classifier: boosting for autism classification. In: International Conference on Medical Image Computing and Computer-Assisted Intervention. Springer, VerlagBerlin, Heidelberg
5. Ecker C et al (2010) Describing the brain in autism in five dimensions—magnetic resonance imaging-assisted diagnosis of autism spectrum disorder using a multiparameter classification approach. J Neurosci 30(32):10612–10623
6. Jiao Y et al (2010) Predictive models of autism spectrum disorder based on brain regional cortical thickness. Neuroimage 50(2):589–599
7. Katuwal GJ, et al (2015) The predictive power of structural MRI in autism diagnosis. In: 2015 37th annual International conference of the IEEE engineering in medicine and biology society (EMBC). IEEE, Milano
8. Ismail M, et al (2017) A new deep-learning approach for early detection of shape variations in autism using structural MRI. In: 2017 IEEE International Conference on Image Processing (ICIP). IEEE, Beijing
9. Xiao X et al (2017) Diagnostic model generated by MRI-derived brain features in toddlers with autism spectrum disorder. Autism Res 10(4):620–630
10. Khalil, A. et al. A new deep-learning approach for early detection of shape variations in autism using structural mr. 2018
11. Ashburner J, Friston KJ (2000) Voxel-based morphometry—the methods. Neuroimage 11(6):805–821
12. Klein A, Andersson J, Ardekani BA, Ashburner J, Avants B, Chiang MC, Parsey RV (2009) Evaluation of 14 nonlinear deformation algorithms applied to human brain MRI registration. Neuroimage 46(3):786-802
13. Dahnke R, Yotter RA, Gaser C (2013) Cortical thickness and central surface estimation. Neuroimage 65:336–348
14. Yotter RA et al (2011) Topological correction of brain surface meshes using spherical harmonics. Hum Brain Mapp 32(7):1109–1124
15. Akshoomoff N et al (2004) Outcome classification of preschool children with autism spectrum disorders using MRI brain measures. J Am Acad Child Adolesc Psychiatry 43(3):349–357
16. Rommelse N, Buitelaar JK, Hartman CA (2017) Structural brain imaging correlates of ASD and ADHD across the lifespan: a hypothesis-generating review on developmental ASD–ADHD subtypes. J Neural Transm 124(2):259–271
17. Qureshi MNI, Lee B (2016) Classification of ADHD subgroup with recursive feature elimination for structural brain MRI. In: 2016 38th Annual International Conference of the IEEE Engineering in Medicine and Biology Society (EMBC). IEEE, Orlando
18. Peng X et al (2013) Extreme learning machine-based classification of ADHD using brain structural MRI data. PLoS One 8(11):e79476
19. Iannaccone R et al (2015) Classifying adolescent attention-deficit/hyperactivity disorder (ADHD) based on functional and structural imaging. Eur Child Adolesc Psychiatry 24(10):1279–1289
20. Igual L et al (2012) Automatic brain caudate nuclei segmentation and classification in diagnostic of attention-deficit/hyperactivity disorder. Comput Med Imaging Graph 36(8):591–600
21. Chang C-W, Ho C-C, Chen J-H (2012) ADHD classification by a texture analysis of anatomical brain MRI data. Front Syst Neurosci 6:66
22. Johnston BA et al (2014) Brainstem abnormalities in attention deficit hyperactivity disorder support high accuracy individual diagnostic classification. Hum Brain Mapp 35(10):5179–5189
23. Zhang B, et al (2017) Classification based on neuroimaging data by tensor boosting. In: 2017 International Joint Conference on Neural Networks (IJCNN). IEEE, Anchorage
24. Wang Z et al (2019) Dilated 3D convolutional neural networks for brain MRI data classification. IEEE Access 7:134388–134398

Publisher's Note

Springer Nature remains neutral with regard to jurisdictional claims in published maps and institutional affiliations.